J Fluoresc (2016) 26:1–9
DOI 10.1007/s10895-015-1713-z

RAPID COMMUNICATION

Fluorescein-*N*-Methylimidazole Conjugate as Cu^{2+} Sensor in Mixed Aqueous Media Through Electron Transfer

Aasif Helal[1] · Hong-Seok Kim[2] · Zain H. Yamani[1] · M. Nasiruzzaman Shaikh[1]

Fluorescence Spectroscopy

<paper review>

Antonio Osamu Katagiri Tanaka
A01212611@itesm.mx

16 Apr 2020

Helal et al. synthesized a fluorescein probe with fluorescein hydrazine and N-methylimidazole. Due to the electron-donating capability of imidazole, makes the probe to produce a green fluorescence emission at 535 nm and specific selection for copper. Cu^{2+} being a paramagnetic cationic species, quenches the fluorescence of the probe upon binding, inhibiting the electron transfer (ET) between the fluorescein and imidazole.

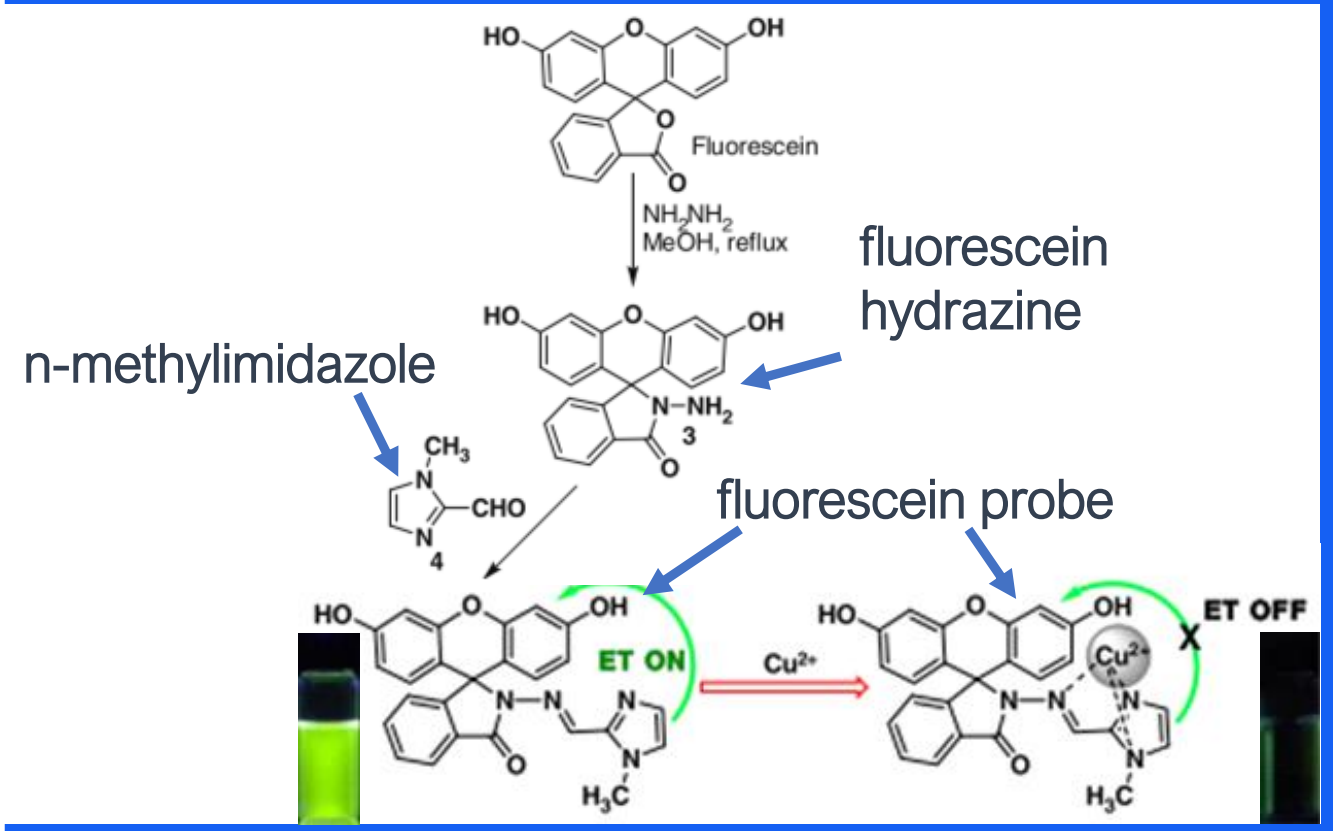

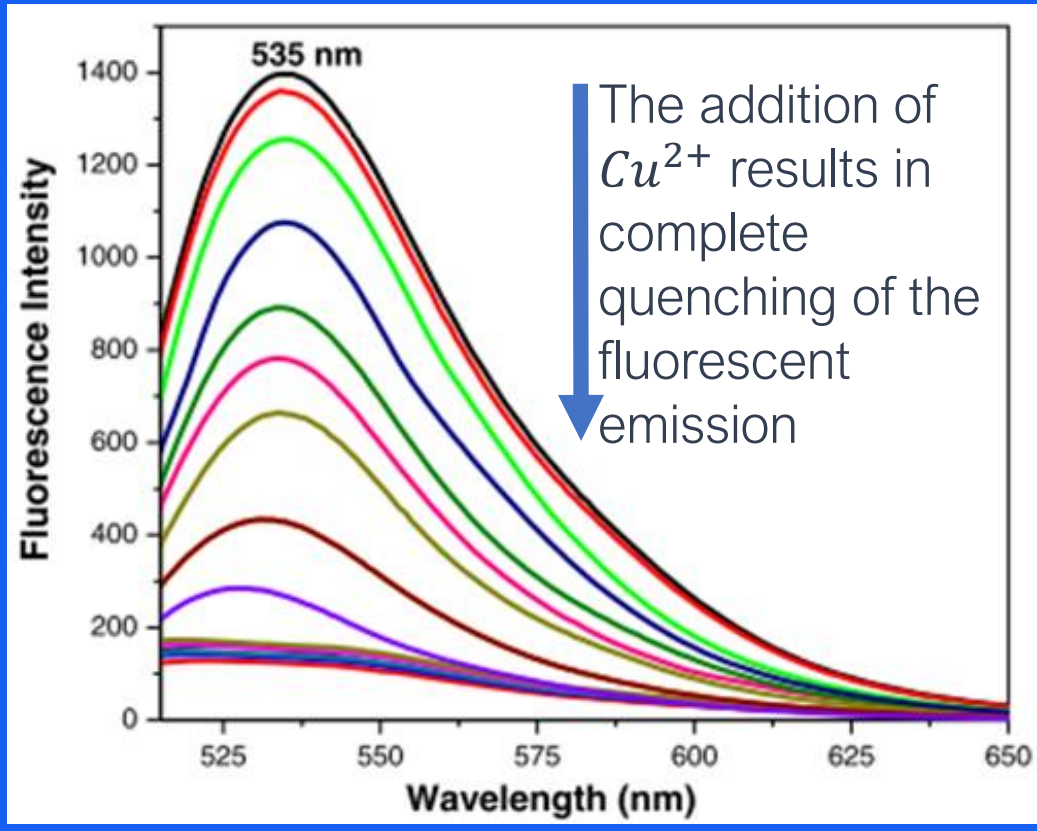

[1] A. Helal, H.-S. Kim, Z.H. Yamani, M. Nasiruzzaman Shaikh, Fluorescein-N-Methylimidazole Conjugate as Cu2+ Sensor in Mixed Aqueous Media Through Electron Transfer, J. Fluoresc. 26 (2016) 1–9. https://doi.org/10.1007/s10895-015-1713-z.

J Fluoresc (2016) 26:1–9
DOI 10.1007/s10895-015-1713-z

RAPID COMMUNICATION

Fluorescein-*N*-Methylimidazole Conjugate as Cu^{2+} Sensor in Mixed Aqueous Media Through Electron Transfer

Aasif Helal[1] · **Hong-Seok Kim**[2] · **Zain H. Yamani**[1] · **M. Nasiruzzaman Shaikh**[1]

Received: 24 September 2015 / Accepted: 26 October 2015 / Published online: 14 November 2015

Abstract A new highly selective, chromogenic, and fluorogenic Cu^{2+} chemosensor, fluorescein-*N*-methylimidazole conjugate **1**, and another fluorescein-*N*-imidazole conjugate **2** were synthesized and investigated by UV-visible and fluorescence spectroscopy. The sensing of Cu^{2+} quenches the emission band of **1** at λ_{max} = 525 nm, with an association constant (K_a = 1.0 x 10^7 M^{-1}) and a stoichiometry of 1:1 in a buffered H_2O: MeOH solution (4:1, pH = 7.4). The Cu^{2+} detection limit for chemosensor **1** is 37 nM. The presence of the *N*-methyl group in **1** increased the Cu^{2+} binding selectivity, resulting in a stronger binding constant and a broader pH working range (pH 5–10) in comparison to **2**. The fluorescence in **1** and **2** is caused by electron transfer phenomenon from the imidazole nitrogen to fluorescein, which is readily inhibited by Cu^{2+} binding.

Keywords Fluorescent chemosensor · Copper ion-selective · Fluorescein-*N*-methylimidazole electron transfer

Introduction

Fluorescent chemosensors are highly valuable as they provide an accurate detection of toxic heavy metal ions with high sensitivity and specificity. They are easily accessible at a lower cost, and offer a rapid tracking of analytes in biological, toxicological, and environmental samples [1, 2]. Copper is the third most essential element for living organisms after iron and zinc [3]. Its effects are diverse and far-ranging, as it serves as an essential cofactor for numerous redox enzymes involved in critical processes such as respiration (e.g., cytochrome c oxidase) [4], electron transfer/substrate oxidation and iron uptake (ceruloplasmin) [5], pigmentation (tyrosinase) [6], neurotransmitter synthesis and metabolism (dopamine β-hydroxylase, peptidylglycine), and handling of dietary amines (copper amine oxidases) [7]. However, unregulated overloading of copper from copper polluted water is linked to human genetic disorders (Menkes and Wilson's diseases) [8], neurodegenerative diseases (e.g. Alzheimer's, Parkinson's, prion, and Huntington's diseases as well as familial amyotrophic lateral sclerosis) [9–13], and metabolic disorders (e.g. obesity and diabetes) [14, 15]. Recently, copper has also been found to regulate cancers [16]. Owing to its widespread use in various industries, the Cu^{2+} species is a significant environmental pollutant. The World Health Organization (WHO) has set the safe limit of copper in drinking water at 2 ppm (31.5 μM) [17]. Thus, the development of chemosensors for the selective analysis of Cu^{2+} with high sensitivity, low detection limit, and quick response is in great demand [18]. Current methods for copper screening, which include atomic absorption spectrometry (AAS) [19], inductively coupled plasma mass spectrometry (ICP-MS) [20], and inductively coupled plasma atomic emission spectrometry (ICP-AES) [21], total reflection X-Ray fluorescence (TXRF) spectrometry, and anodic stripping voltammetry (ASV) [22, 23], often require expensive and sophisticated instrumentation or complex sample preparation steps. On the other hand, Cu^{2+} can also be detected using small molecular chemosensors based on rhodamine Schiff base [24], novel rhodamine hydrazine [25], pyridoxal moiety

Electronic supplementary material The online version of this article (doi:10.1007/s10895-015-1713-z) contains supplementary material, which is available to authorized users.

✉ Aasif Helal
aasifh@kfupm.edu.sa

[1] Center of Research Excellence in Nanotechnology, King Fahd University of Petroleum and Minerals, Dhahran 31261, Saudi Arabia

[2] Department of Applied Chemistry, Kyungpook National University, Daegu 702-701, Republic of Korea

[26], as well as novel coumarin [27] and thiazole-derived groups [28, 29].

Among highly fluorescent dyes, xanthene-based rhodamine and fluorescein dyes have attracted considerable interests from chemists owing to their excellent photophysical properties [30]. The fluorescein structure is an ideal model for the construction of fluorescent chemosensors because of the easy of synthesis and functionalization [31], excitation and emission wavelengths in the visible region with a high fluorescence quantum yield [32–35], excellent biocompatibility, high molar extinction coefficient, and high photostability and water solubility [36, 37].

Imidazole is widely used as a building block in many fields such as medicine [38], biology [39], electronic and optical materials [40], ionic liquids [41], and chemosensors [42–45]. It is a π-electron-rich heteroaromatic molecule with electron density concentrated on the N-atoms. Moreover, imidazole shows excellent coordination properties toward metal ions [46], and various substituted imidazoles form complexes with many metal ions, in which the electrons are donated by the pyridinic N-atom. Imidazole and its functionalized derivatives have been applied in environmental monitoring, industrial process control, metalloneurochemistry, and biomedical diagnostics because of their bioactivities [42–46].

Schiff bases are well known as good metal ion ligands and they can be easily synthesized. Thus, Schiff base derivatives, incorporated with a fluorescent moiety as the signaling unit and imidazole as the binding unit, are appealing as optical sensing tools for metal ions [47–49]. However, there is a lack of precedence on the use of fluorescein-imidazole conjugate for metal ion sensing. Herein, we spectrophotometrically and spectrofluorometrically investigated a new Schiff base compound (**1**) (Scheme 1), consisting of fluorescein hydrazone and *N*-methylimidazole, as a chemosensor for metal ions. The fluorescein hydrazone and (NH)-imidazole conjugate (**2**) was also prepared to study the effect of the methyl group on metal binding selectivity. The reversible, highly selective chromogenic and fluorogenic responses of **1**, upon the addition of Cu^{2+} in a mixed aqueous solution containing 4-(2-hydroxyethyl)-1-piperazineethanesulfonic acid (HEPES) buffer (10 mM, pH 7.4), and its binding characteristics (in competition with other cations) are reported.

Experimental Section

General Methods

Melting points were determined using a Thomas-Hoover capillary melting point apparatus and are uncorrected. ^{1}H and ^{13}C NMR spectra were recorded on a JEOL 500 MHz spectrometer using Me_4Si as the internal standard. The HR-FAB mass was determined at the KBSI Daegu branch South Korea. UV–vis

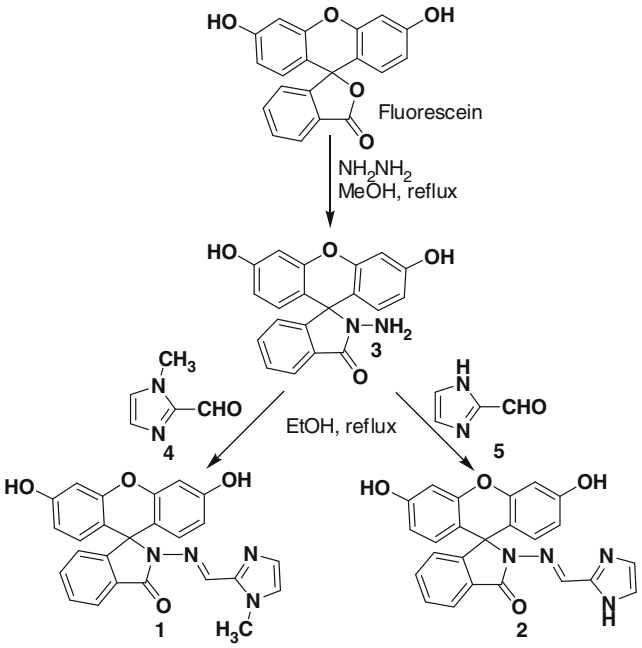

Scheme 1 Synthesis of **1** and **2**

absorption spectra were obtained using a Jasco V-670 spectrophotometer. Fluorescence spectra were measured using a Horiba, Fluorolog-3 fluorescence spectrophotometer, equipped with a xenon discharge lamp and 1 cm quartz cells with slit width 5 nm. All of the measurements were carried out at 298 K.

Analytical grade absolute ethanol and methanol were purchased from Merck. Deionized water (double distilled) was used throughout the experiment as the aqueous media. All other materials used for synthesis were purchased from Aldrich Chemical Co. and used without further purification. Compounds **3**, **4**, and **5** were prepared in accordance with the literature procedure [47–49]. The solutions of metal ions were prepared from their nitrate and chloride salts (analytical grade), and subsequently diluted to prepare working solutions. HEPES buffer solutions at different pH values were prepared using appropriate amounts of HEPES and KOH (all of analytical grade) under adjustment by a Mettler Toledo pH meter.

Determination of Quantum Yield

The fluorescence quantum yields were determined using fluorescein as a reference, with a known Φ value of 0.89 in EtOH [50]. The quantum yield was calculated according to the following equation (1):

$$\Phi_S/\Phi_R = (A_S/A_R) \times (Abs_R/Abs_S) \times \left(\eta^2{}_S/\eta^2{}_R\right) \qquad (1)$$

where Φ is the fluorescence quantum yield; A is the integral of fluorescence spectrum; Abs is the corresponding absorbance at the excitation wavelength; η is refractive index; and the subscripted letters S and R denote sample and reference, respectively.

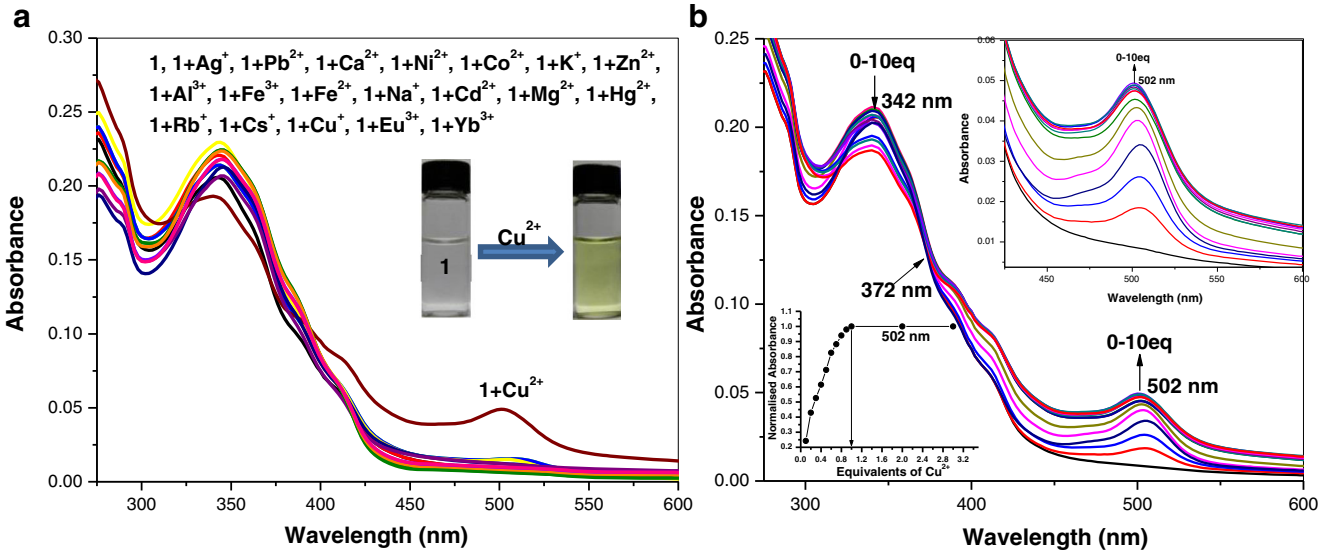

Fig. 1 UV-Vis spectra of **1** (20 μM) **a** with different cations (10 equivalents), **b** upon the addition of $Cu(NO_3)_2$ (200 μM) in H_2O:MeOH (4:1) containing HEPES buffer (10 mM, pH 7.4). Inset: **a** visible color change from colorless to light yellow. **b** Mol ratio plot of absorbance at 502 nm

Synthesis

Synthesis of 1

Fluorescein hydrazide (**3**, 0.5 g, 1.4 mmol) and *N*-methylimidazole-2-carbaldehyde **4** (0.191 g, 1.7 mmol) were suspended in 10 mL of ethanol. The mixture was refluxed for 12 h with stirring, resulting in the formation of a yellow precipitate. The precipitate was separated by filtration and washed with 3 × 10 mL of ethanol. After drying, a yellowish solid was obtained in 85 % yield. mp. 208–210 °C (CH_2Cl_2-hexane); ^{1}H NMR (400 MHz, DMSO-d_6), δ (ppm): 3.74 (s, 3 H), 6.38 (d, J = 6.8 Hz, 3 H), 6.42–6.48 (m, 3 H), 6.59 (d, J = 1.6 Hz, 2 H), 6.96 (d, J = 6.4 Hz, 1 H), 7.63 (t, J = 5.6 Hz, 1 H), 7.69 (t, J = 5.6 Hz, 1 H), 7.77 (d, J = 6.8 Hz, 1 H), 8.24 (s, 1 H), 9.67 (s, 2 H). ^{13}C NMR (100 MHz, DMSO-d_6), δ (ppm): 33.82, 65.83, 102.63, 110.1, 112.29, 122.68, 123.59, 128.14, 128.37, 128.47, 128.5, 128.72, 129.33, 129.76, 132.96, 133.3, 151.75, 152.45, 152.59, 158.36, 158.38, 158.86, 159, 164.37, 165.94 (Fig. S1 and S2). Anal Calcd for 1, $C_{25}H_{18}N_4O_4$: C, 68.49; H, 4.14; N, 12.78, Found: C, 68.38; H, 4.15; N, 12.65; HR-mass Calcd for: $C_{25}H_{18}N_4O_4$ $[M + H]^+$: 439.1406; Found: m/z 439.1405 (Fig. S3).

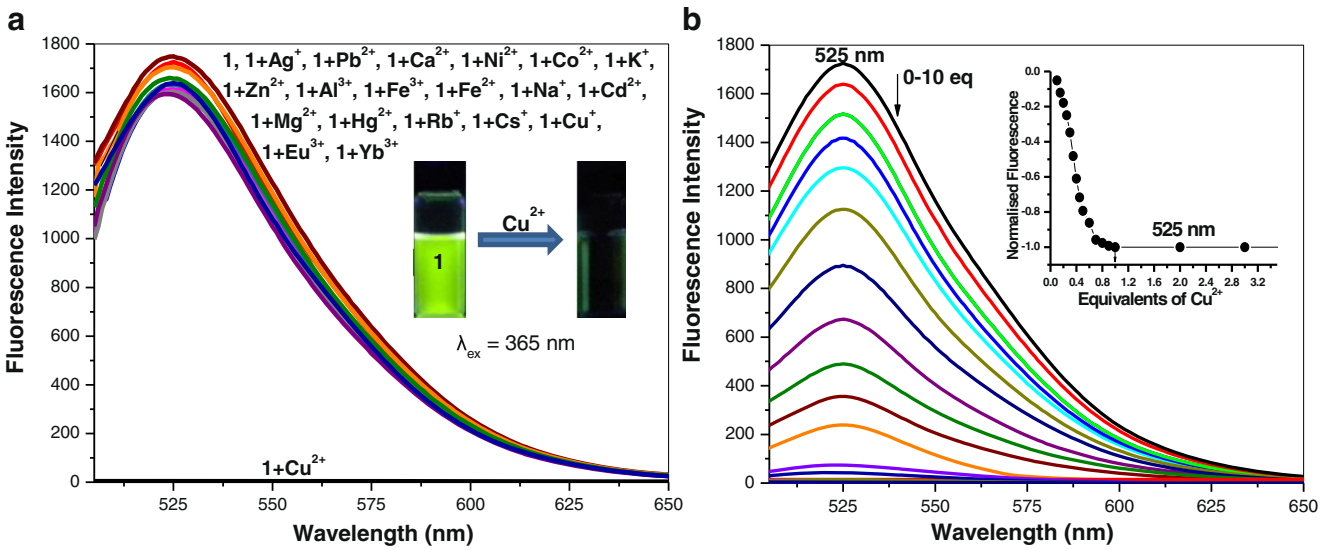

Fig. 2 Fluorescence spectra of **1** (0.2 μM) **a** with different cations (10 equivalents) **b** as a function of added $Cu(NO_3)_2$ in H_2O:MeOH (4:1) containing HEPES buffer (10 mM, pH 7.4). (λ_{ex} = 502 nm). Inset: **a** Fluorogenic change from green to colorless upon illumination at 365 nm. **b** Mol ratio plot of emission at 525 nm

Synthesis of 2

Fluorescein hydrazide (**3**, 0.4 g, 1.2 mmol) and imidazole-2-carbaldehyde (**5**, 0.133 g, 1.4 mmol) were suspended in 10 mL of ethanol. The mixture was refluxed for 12 h with stirring, resulting in the formation of a yellowish precipitate. The precipitate was separated by filtration and washed with 3 × 10 mL of ethanol. After drying, a yellowish solid in 87 % yield was obtained. mp. 217–219 °C (CH_2Cl_2-hexane); ^{1}H NMR (400 MHz, DMSO-d_6), δ (ppm): 6.46 (dd, J = 8.8 Hz, 2.2 Hz, 3 H), 6.53 (d, J = 6.8 Hz, 3 H), 6.67 (d, J = 2.0 Hz, 2 H), 7.02 (d, J = 6.0 Hz, 1 H), 7.13 (s, NH, 1 H), 7.53 (t, J = 6.0 Hz, 1 H), 7.58 (t, J = 5.6 Hz, 1 H), 7.91 (d, J = 6.0 Hz, 1 H), 8.06 (s, 1 H), 9.6 (s, 2 H). ^{13}C NMR (100 MHz, DMSO-d_6), δ (ppm): 64.47, 102.86, 108.93, 109.84, 112.02, 11,268, 123.33, 126.74, 127.57, 128.33, 128.44, 128.7, 129.01, 129.07, 132.69, 134.37, 137.24, 142.17, 145.52, 151.42, 151.94, 152.33, 158.74, 164.33 (Fig. S4 and S5). Anal Calcd for 2, $C_{24}H_{16}N_4O_4$: C, 67.92; H, 3.80; N, 13.20; Found: C, 67.67, H 3.95; N, 13.02; HR-mass Calcd for: $C_{24}H_{16}N_4O_4$ $[M + H]^+$: 425.1172; Found: m/z 425.1169 (Fig. S6).

Cu^{2+}–1 Complex A mixture of **1** (100 mg, 0.23 mmol) and $Cu(NO_3)_2{\cdot}3H_2O$ (62 mg, 0.28 mmol) in methanol (10 mL) was refluxed for 8 h. The mixture was cooled to room temperature and the precipitated complex was filtered. The filtered cake was washed thoroughly with water and ethanol, followed by drying under vacuum to give the copper-bound complex (95 mg, 82 % yield). HR-FAB Mass: calcd for ($C_{25}H_{18}O_4N_4$.Cu) 501.0624; found: 501.0621 (Fig. S7).

Result and Discussion

Compound **1** was designed to bind metal ions via the carbonyl oxygen, imino N group and the imidazole N atoms serving as electron donors. Scheme 1 outlines the syntheses of **1** and **2**, based on the respective reactions of **3** with *N*-methylimidazole-2-carbaldehyde (**4**) and methylimidazole-2-carbaldehyde (**5**) in ethanol. Both compounds were prepared in good yields and their structures were confirmed using ^{1}H and ^{13}C NMR, mass spectrometry, and elemental analysis (Supporting information S1, S2, S3, and S4). The formation of imine could be easily identified via the =C-H proton singlet peak at δ 8.24 and 8.06 ppm for compounds **1** and **2** respectively. Compounds **1** and **2** could be easily distinguished from one another via the presence of a singlet methyl proton (**N-CH$_3$**) peak at δ 3.74 ppm in **1** and the **NH** singlet peak at δ 7.13 ppm in **2**. The hydroxyl protons of the fluorescein appeared as a singlet at δ 9.67 and 9.60 ppm for **1** and **2**, respectively.

Table 1 Comparisons of the absorption, emission, and binding properties of sensors **1** and **2** in H_2O:MeOH (4:1)

	1	**1** + Cu^{2+}	**2**	**2** + Cu^{2+}
λ_{max} (nm)	342	342, 502	330	330, 502
log ε	4.1	4.0, 3.4	3.9	3.8, 3.2
λ_{em} (nm)	525	No fluorescence	535	535
I/I_0		0.0		0.2
Φ[a]	0.32		0.19	
K_a (M^{-1})		1.0×10^7		1.3×10^6

[a] Quantum yields were obtained using Fluorescein in EtOH as standard

All the absorption and emission studies were carried out in a mixed aqueous solution of water and methanol (4:1) containing HEPES buffer (10 mM, pH 7.4) at a concentration of 20 μM and 0.2 μM, respectively. The sensor **1** exhibited an absorption peak at 342 nm, which was ascribed to the absorption of the xanthene moiety [51, 52]; however, there was no observable absorption in the visible region, indicating that probe **1** exists in the lactam form while in solution. However, upon the addition of Cu^{2+} into the solution of **1**, a new red-shifted absorption band at 502 nm was gradually enhanced, while the absorption band at 342 nm decreased synchronously with an isobestic point at 372 nm as shown in Fig. 1b and the solution color changed from colorless to light yellow (Fig. 1a, inset). The peak at 502 nm in the UV-vis spectra was attributed to the ring opening of the spirolactam, which was triggered by the binding of the Cu^{2+} species. The respective absorption bands at 502 nm increased linearly, up to 1 equiv. of Cu^{2+} (Fig. 1b, inset), indicating the formation of a 1:1 complex with a strong binding affinity. The Job's plot of **1** with Cu^{2+} also confirmed the formation of a 1:1 complex (Fig. S8). Under these conditions, the observed response was selective for Cu^{2+} ions. The addition of other common metals cations (10 equiv), particularly the alkali and alkaline earth metals, as well as transition metals, produce minimal or no appreciable spectral changes (Fig. 1a).

Subsequently, emission studies were carried out by adding 10 equiv. of various biologically and non-biologically relevant metal cations into a H_2O-MeOH (4:1) solution of **1** (0.2 μM), and their complexation abilities were studied by fluorescence.

Compound **1**, when excited at 502 nm, gave a strong fluorescence emission peak at 525 nm. With the addition of Cu^{2+}, the emission was completely quenched and none of the other cations induced such distinct emission shift or quenching

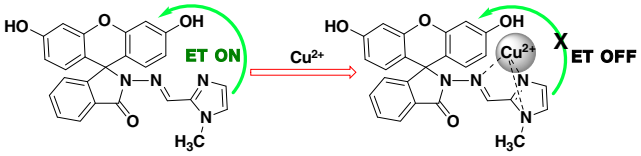

Fig. 3 The proposed scheme for complexation of sensor **1** with Cu^{2+} ion

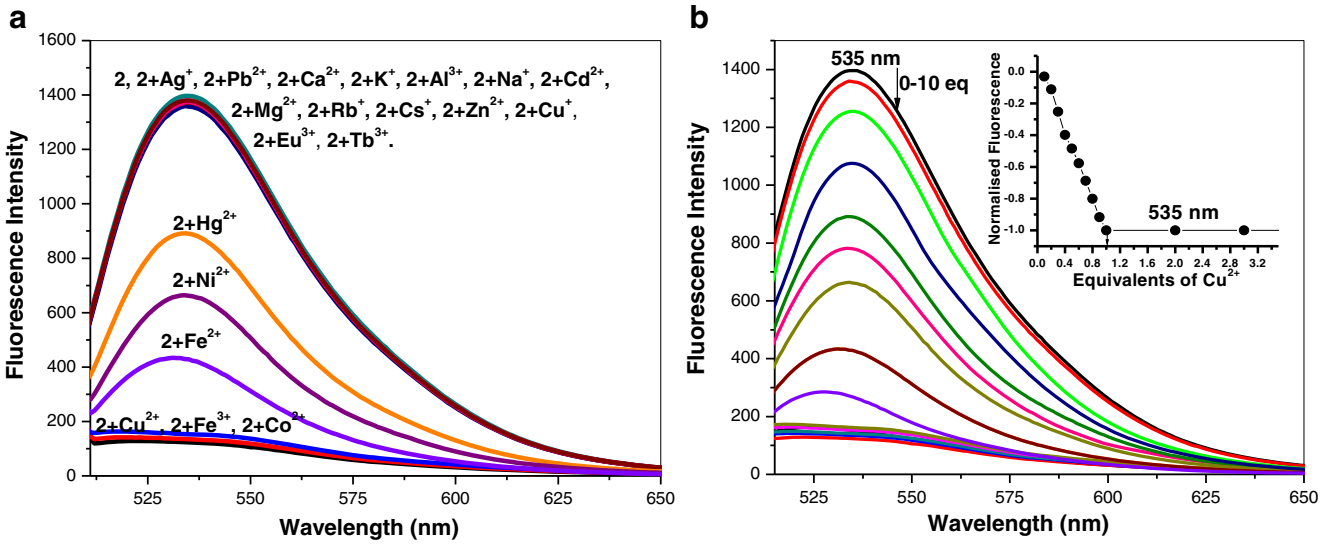

Fig. 4 Fluorescence spectra of **2** (0.2 μM) **a** with different cations (10 equivalents) **b** as a function of added $Cu(NO_3)_2$ in H_2O:MeOH (4:1) containing HEPES buffer (10 mM, pH 7.4). (λ_{ex} = 502 nm). Inset: Mol ratio plot of emission at 535 nm

(Fig. 2a). Additionally, the green fluorescence was completely quenched on illumination at 365 nm (Fig. 2a, inset). Fluorescence titration of **1** with Cu^{2+} was carried out in H_2O-MeOH (4:1) at a concentration of 0.2 μM. The addition of Cu^{2+} to the solution of **1** resulted in a complete quenching of the fluorescent emission and the peak at 525 nm (Φ = 0.32, Table 1) was "*switched off*" when excited at 502 nm (Fig. 2b). The relatively long excitation (502 nm) and emission (525 nm) wavelengths of **1** can prevent autofluorescence interference from native cellular species, and limit potential damage to living biological samples [53–56]. The reabsorption of fluorescence in this case can be avoided due to the dilute concentration (0.2 μM), small area of overlapping of the absorption and the fluorescence peaks, and the molar absorptivity is low in the overlapping spectral region [57]. The fluorescein moiety is weakly fluorescent in solution with no absorption in the visible region, owing to the predominance of the ring-closed spirolactam form, which was confirmed by ^{13}C NMR signals at δ 65.83 and δ 64.47 ppm for compounds **1** and **2**, respectively [36, 37]. The green fluorescence in **1** and **2** arises as a result of electron transfer (ET) phenomenon from imidazole's nitrogen to the fluorescein ring (i.e., ET is "*switched on*") (Fig. 3) [42–45].

Cu^{2+} being a paramagnetic cationic species, with open shell d-orbitals, quenches the fluorescence of **1** upon binding, presumably due to the ET from imidazole to the metal cation that inevitably inhibits the ET between the fluorescein and imidazole (i.e ET is "*switched off*"). This provides a very fast and efficient nonradiative decay of the excited state that result in quenching [42–45, 58]. The peak at 525 nm showed a linear diminution with increasing Cu^{2+} concentration when the ratio of Cu^{2+} to **1** was ≤1:1. When a 1:1 ratio was reached, however, a higher Cu^{2+} concentration no longer led to any further emission changes (Fig. 2b. inset) [59, 60].

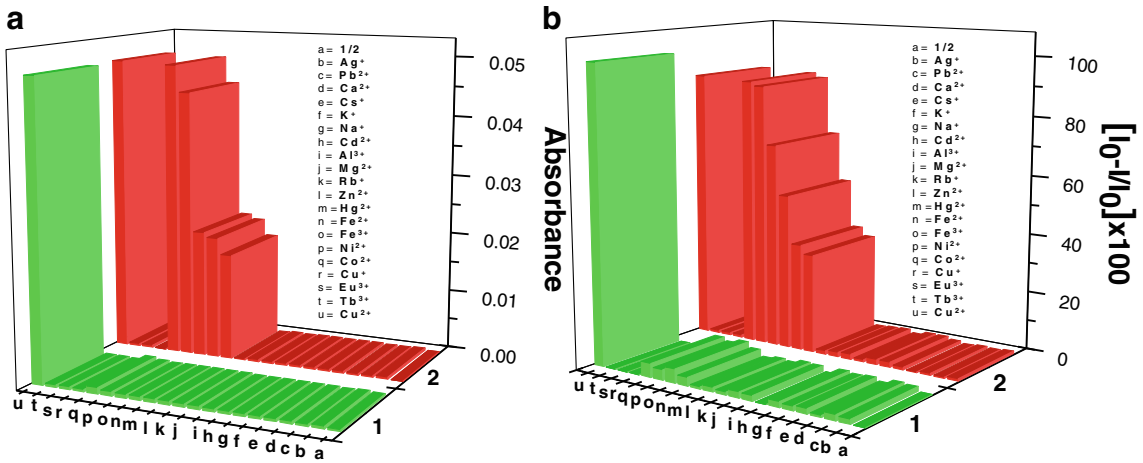

Fig. 5 Comparative **a** absorption and **b** relative fluorescence spectra of **1** and **2** (0.2 μM) with different cations (10 equivalents) in H_2O:MeOH (4:1) containing HEPES buffer (10 mM, pH 7.4)

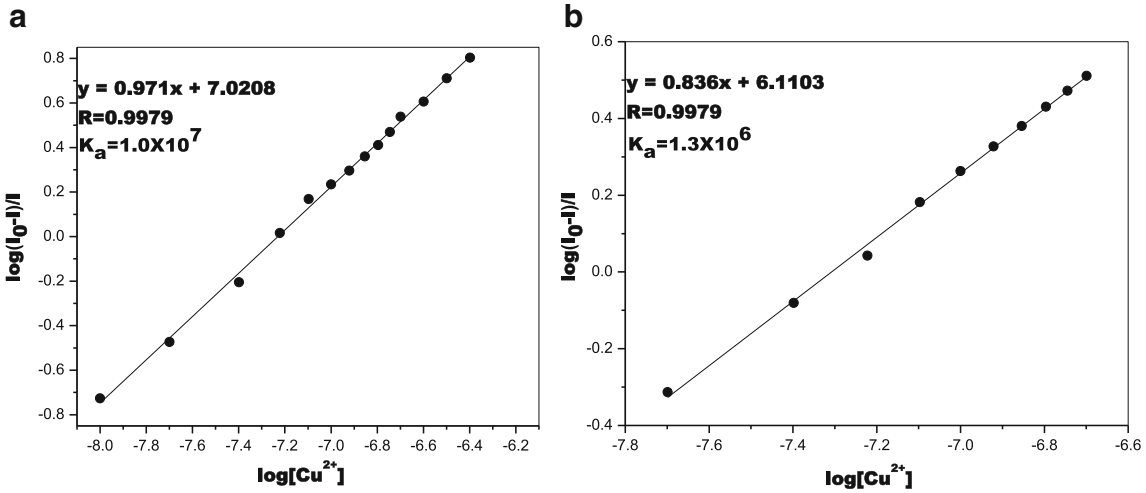

Fig. 6 Stern–Volmer plot of **a 1** and **b 2** obtained by plotting log $(I_0\text{-}I)/I$ as a function of log[Cu^{2+}] in H_2O:MeOH (4:1) containing HEPES buffer (10 mM, pH 7.4). (λ_{ex} = 502 nm for **1** and **2**)

To evaluate the selectivity and tolerance of **1** for Cu^{2+} over other metal cations, 10 eq. of different metal cations were added to 0.2 μM solutions of **1**. For Cu^{2+}, the molecular fluorescence was quenched to a maximum level, therefore demonstrating high molecular sensitivity. Nevertheless, there was no quenching with any other metal ions as shown in Fig. 2a. The observed selectivity is rooted in the fact that although transition metals do not differ much in size, but they can establish coordinative interactions at very different energies. Such behavior can be used for discriminative purposes, especially for fluorescent sensing [61]. This phenomenon is consistent with copper that occurs highest on the Irving–Williams series [62]. Copper(II) has a particularly high thermodynamic affinity for the typical imino nitrogen, carbonyl group of the amide, and the imidazole nitrogen; with fast metal-to-ligand binding kinetics that are not exhibited by other transition metal ions. Competitive binding experiments between different metal ions (10.0 eq.) and Cu^{2+} ion (1.0 eq.) showed that the quenching of Cu^{2+} by **1** was not disrupted by any other species (Fig. S9). It was also found that **1** has a detection limit of 0.037 μM and thus, is able to effectively sense the Cu^{2+} concentration in the blood system and in drinking water (Fig. S10) [31].

In order to study the effect of the *N*-methyl group on the imidazole ring, we prepared compound **2** and studied its absorption and emission properties with different metal cations. The absorption spectra of **2** showed peaks at 330 nm resulting from the absorption of the xanthene moiety [50, 51] and it was selective to Co^{2+}, Fe^{3+}, and Cu^{2+} (Fig. S11). Fluorescence spectra of **2** in H_2O-MeOH (4:1 *v*/*v*) showed the emission peak at 535 nm (Φ = 0.19, Table 1) corresponding to the ET from imidazole to the fluorescein moiety. On addition of different metal cations to **2** Fe^{3+}, Co^{2+}, and Cu^{2+} completely quenched the fluorescence signal of **2**, with Hg^{2+}, Fe^{2+}, and Ni^{2+} ions achieving partial quenching (Fig. 4a). In fluorescence titration, the addition of Cu^{2+} up to 1 equiv. completely quenched the emission peak, but no further quenching occurred thereafter (tested up to 10 equiv) (Fig. 4b). The fluorescence titration showed that the complexation of 2 and Cu^{2+} occurs at a 1:1 ratio. Thus, we deduced that the introduction of the electron-donating methyl group on the imidazole ring increases the electron-donating capability of

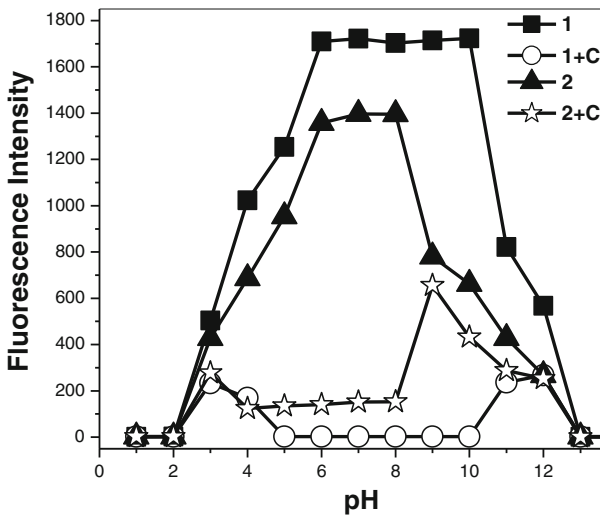

Fig. 7 Effect of pH on the emission intensities of **1** and **2**, and their Cu^{2+} complexes in H_2O:MeOH (4:1) containing HEPES buffer (10 mM, pH 7.4). (λ_{ex} = 502 nm for **1** and **2**)

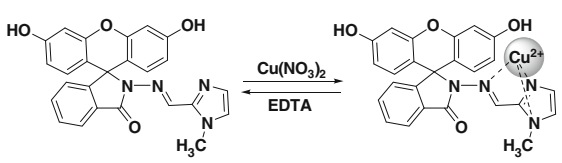

1: λ_{max} = 342 nm, λ_{em} = 525 nm

1 + Cu^{2+}: λ_{max} = 502, 342 nm, λ_{em} = no fluorescence

Scheme 2 Reversibility of **1** toward Cu^{2+}

imidazole, which makes compound **1** more selective to Cu^{2+} than **2** (Fig. 5) [45].

Based on the fluorescence titration spectra of **1** and **2** with Cu^{2+}, the job plot of **1,** and the high resolution (HR)-mass of the **1**-$\mathbf{Cu^{2+}}$ complex, we found that the binding of **1** and **2** with Cu^{2+} follow a 1:1 stoichiometric complex formation in the aqueous MeOH (4:1of H_2O-MeOH) solution. Thus, it can be assumed that the fluorescence quenching of **1** and **2** by Cu^{2+} occurs via a static quenching mode owing to the formation of a non-fluorescent complex in the ground state [48]. In the case of a static quenching, the Stern–Volmer plot is linear and it is used to calculate the respective binding constants of **1** and **2** with Cu^{2+} [58, 59]. From the Stern-Volmer linear plot (Fig. 6a and 6b), the binding constant (K_a) of **1** and **2** with Cu^{2+} were calculated to be $1.0x10^7$ and 1.3×10^6 M^{-1} (Error limits ≤10 %) [59, 60]. The binding constant of **1** with Cu^{2+} was ten times greater than that of compound **2** owing to the electron donating nature of the methyl group on the imidazole ring (Table 1) [45].

For environmental and physiological applications, chemosensors should operate in a wide range of pH. As such, the effects of pH on the emission intensities of **1** and **2**, in the absence and presence of Cu^{2+} ions, were investigated in the pH range of 2.0–12.0 (Fig. 7). Fluorescein exists in a closed, colorless, and non-fluorescent spirocyclic form at neutral and basic pH. In both **1** and **2** decreasing the pH value protonates the nitrogen of the imidazole ring and this inhibits the ET to fluorescein, resulting in decreasing fluorescence. Compounds **1** and **2** showed maximum fluorescence intensities at pH 5.0 and 6.0, respectively, and they remained unchanged until the pH value increased to 10.0 (for compound **1**) and 8.0 (for compound **2**). At higher pH values (> 10.0 in case of **1** and >8.0 in case of **2**), the fluorescence intensity decreased due to the enhancement of negative charge density on the imidazole ring and formation of phenolate on the fluorescein core (Figs. S-12a, S-12b) [36, 37, 47–49]. It was shown that the amount of quenching (based on fluorescence intensity) associated with the Cu^{2+} complexes of **1** and **2** increases with ascending pH values, reaching their maximum efficiency at pH 5.0 for **1** + Cu^{2+} and pH 6.0 for **2** + Cu^{2+}. The quenching process was eventually disrupted at pH 10.0 and 8.0 for complexes **1** + Cu^{2+} and **2** + Cu^{2+}, respectively. As the pH increases, the fluorescence intensities of **1**, **2** and their respective Cu^{2+} complexes become closer, probably owing to the favorable formation of a Cu^{2+} based hydroxo-complex under such conditions (Figs. S-13a, S-13b) [47–49]. Thus, chemosensors **1** and **2** displayed virtually no physiological pH-sensitivity and their fluorescence "*on–off*" can be controlled by Cu^{2+} ion binding within the pH range of 5.0 to 10.0 and 6.0 to 8.0, respectively.

The chemical reversibility of Cu^{2+}-induced fluorescence response of **1** in the buffered H_2O:MeOH (4:1) solution was investigated. When an aqueous MeOH solution of EDTA (2.0 μM) was added to the complexed solution of **1** (0.2 μM) and Cu^{2+} ions (2.0 μM), the fluorescence signal at 525 nm was instantly recovered. The solution turned from light yellow to colorless (a reversal of Fig. 1a, inset) with the disappearance of the absorption peak at 502 nm. The introduction of the EDTA chelator immediately captured the sensor-bound Cu^{2+}, proving that the binding of **1** with Cu^{2+} is a chemically reversible process (Scheme 2). Thus, **1** could potentially serve as a recyclable chemical tool in materials sensing.

Conclusion

In conclusion, we have developed a new highly efficient, reversible chemosensor (**1**) based on a fluorescein-*N*-methylimidazole conjugate for Cu^{2+} sensing in a H_2O-MeOH (4:1) solution containing HEPES buffer (10 mM, pH 7.4). Fluorescein-*N*-methylimidazole produces a green fluorescence emission due to ET from imidazole to the fluorescein ring. On the addition of copper cations, the ET is *switched off*, resulting in fluorescence quenching. When compared to fluorescein-imidazole conjugate **2**, we found that the presence of a methyl group on the imidazole ring of sensor **1** improves the selectivity and binding of Cu^{2+}.

Acknowledgments The authors gratefully acknowledge the Center of Research Excellence in Nanotechnology (CENT) in King Fahd University of Petroleum and Minerals for providing funds and availing its facilities for analysis and Center of Research Excellence in Renewable Energy, King Fahd University of Petroleum and Minerals for providing us with the Spectrofluorometer for analysis.

References

1. Valeur B, Leray I (2000) Design principles of fluorescent molecular sensors for cation recognition. Coord Chem Rev 205:3–40
2. Yoon J, Kim SK, Singh NJ, Kim KS (2006) Imidazolium receptors for the recognition of anions. Chem Soc Rev 35:355–360
3. Lippard SJ, Berg JM (1994) Principles of bioinorganic chemistry. University Science Books, Mill Valley, CA
4. Ghosh A, Trivedi PP, Timbalia SA, Griffin AT, Rahn JJ, Chan SS, Gohil VM (2014) Copper supplementation restores cytochrome c oxidase assembly defect in a mitochondrial disease model of COA6 deficiency. Hum Mol Genet 23:3596–3606
5. Hellman NE, Gitlin JD (2002) Ceruloplasmin metabolism and function. Annu Rev Nutr 22:439–458
6. Olivares C, Solano F (2009) New insights into the active site structure and catalytic mechanism of tyrosinase and its related proteins. Pigm Cell Melanoma Res 22:750–760
7. Klinman JP (2003) The multi-functional topa-quinone copper amine oxidases. Biochim Biophys Acta 1637:131–137
8. Huster D (2014) Introduction to human disorders of copper metabolism. Ann N Y Acad Sci 1314:37–44
9. Savelieff MG, Lee S, Liu Y, Lim MH (2013) Untangling amyloid-β, tau, and metals in Alzheimer's disease. ACS Chem Biol 8:856–865

10. Matlack KE, Tardiff DF, Narayan P, Hamamichi S, Caldwell KA, Caldwell GA, Lindquist S (2014) Clioquinol promotes the degradation of metal-dependent amyloid-β (Aβ) oligomers to restore endocytosis and ameliorate Aβ toxicity. Proc Natl Acad Sci U S A 111:4013–4018
11. Vonk WI, Kakkar V, Bartuzi P, Jaarsma D, Berger R, Hofker MH, Klomp LW Wijmenga C, Kampinga HH, Sluis B van de (2014) The copper metabolism MURR1 domain protein 1 (COMMD1) modulates the aggregation of misfolded protein species in a client-specific manner. PLoS One 9: 924–928
12. McDonald AJ, Dibble JP, Evans EG, Millhauser GL (2014) A new paradigm for enzymatic control of α-cleavage and β-cleavage of the prion protein. J Biol Chem 289:803–813
13. Xiao G, Fan Q, Wang X, Zhou B (2013) Huntington disease arises from a combinatory toxicity of polyglutamine and copper binding. Proc Natl Acad Sci U S A 110:14995–15000
14. Burkhead JL, Lutsenko S (2013) The Role of Copper as a Modifier of Lipid Metabolism. In: Baez R. V. (ed) Lipid Metabolism, InTech, ISBN: 978-953-51-0944-0
15. Nielsen TS, Jessen N, Jorgensen JO, Moller N, Lund S (2014) Dissecting adipose tissue lipolysis: molecular regulation and implications for metabolic disease. J Mol Endocrinol 52:R199–R222
16. Brady DC, Crowe MS, Turski ML, Hobbs GA, Yao X, Chaikuad A, Knapp S, Xiao KS, Campbell L, Thiele DJ, Counter CM (2014) Copper is required for oncogenic BRAF signalling and tumorigenesis. Nature 509:492–496
17. WHO guidelines values for chemicals that are of health significance in drinking water, Guidelines for Drinking Water Quality, WHO, Geneva, 3rd Edn, 2008.
18. Krämer R (1998) Fluorescent chemosensors for Cu^{2+} ions: fast, selective, and highly sensitive. Angew Chem Int Ed 37:772–773
19. Pourreza N, Hoveizavi R (2005) Simultaneous preconcentration of Cu, Fe and Pb as methylthymol blue complexes on naphthalene adsorbent and flame atomic absorption determination. Anal Chim Acta 549:124–128
20. Becker JS, Zoriy MV, Pickhardt C, Palomero-Gallagher N, Zilles K (2005) Imaging of copper, zinc, and other elements in thin section of human brain samples (hippocampus) by laser ablation inductively coupled plasma mass spectrometry. Anal Chem 77:3208–3216
21. Otero-Romaní J, Moreda-Piñeiro A, Bermejo-Barrera A, Bermejo-Barrera P (2005) Evaluation of commercial C18 cartridges for trace elements solid phase extraction from seawater followed by inductively coupled plasma-optical emission spectrometry determination. Anal Chim Acta 536:213–218
22. Stankovic D, Roglic G, Mutic J, Andjelkovic I, Markovic M, Manojlovic D (2011) Determination of copper in water by anodic stripping voltammetry using Cu-DPABA–NA/GCE modified electrode. Int J Electrochem Sci 6:5617–5625
23. Twining B, Baines S, Fisher N, Jacobsen C, Maser J (2003) Quantification and localization of metal within natural plankton cells using a synchrotron x-ray fluorescence microprobe. J Phys IV 104:435–438
24. Wang M, Zhang D, Li M, Fan M, Ye Y, Y-f Z (2013) A rhodamine-cyclen conjugate as chromogenic and fluorescent chemosensor for copper ion in aqueous media. J Fluoresc 23:417–423
25. Kim HN, Lee MH, Kim HJ, Kim JS, Yoon J (2008) A new trend in rhodamine-based chemosensors: application of spirolactam ring-opening to sensing ions. Chem Soc Rev 37:1465–1472
26. Mandal S, Mandal SK, Khuda-Bukhsh AR, Goswami S (2015) Pyridoxal based fluorescent chemosensor for detection of copper (II) in solution with moderate selectivity and live cell imaging. J Fluoresc 25:1–11
27. Jung HS, Kwon PS, Lee JW, Kim JI, Hong CS, Kim JW, Yan SH, Lee JY, Lee JH, Joo T, Kim JS (2009) Coumarin-derived Cu^{2+}-selective fluorescence sensor: synthesis, mechanisms, and applications in living cells. J Am Chem Soc 131:2008–2012
28. Helal A, Rashid MHO, Choi CH, Kim H-S (2011) Chromogenic and fluorogenic sensing of Cu^{2+} based on coumarin. Tetrahedron 67:2794–2802
29. Helal A, Kim S, Kim H-S (2011) Sensing of cyanide using highly selective thiazole-based Cu^{2+} chemosensor. Bull Kor Chem Soc 32: 3123–3126
30. Zheng H, Zhan X-Q, Biana Q-N, Zhanga X-J (2013) In vivo monitoring of hydrogen sulfide using a cresyl violet-based ratiometric fluorescence probe. Chem Commun 49:429–447
31. Duan Y, Liu M, Sun W, Wang M, Liu S, Li Q (2009) Recent progress on synthesis of fluorescein probes. Mini Rev Org Chem 6:35–43
32. Zhou Y, Li J, Chu K, Liu K, Yao C, Li J (2012) Fluorescence turn-on detection of hypochlorous acid via HOCl-promoted dihydrofluorescein-ether oxidation and its application in vivo. Chem Commun 48:4677–4679
33. Xiong XQ, Song FL, Chen GW, Sun W, Wang JY, Gao P (2013) Construction of long-wavelength fluorescein analogues and their application as fluorescent probes. Chem Eur J 19:6538–6545
34. An JM, Yan MH, Yang ZY, Li TR, Zhou QX (2013) A turn-on fluorescent sensor for Zn(II) based on fluorescein-coumarin conjugate. Dyes Pigments 99:1–5
35. Kim HJ, Park JE, Choi MG, Ahn S, Chang SK (2010) Selective chromogenic and fluorogenic signalling of Hg^{2+} ions using a fluorescein-coumarin conjugate. Dyes Pigments 84:54–58
36. Egawa T, Koide Y, Hanaoka K, Komatsu T, Teraia T, Nagano T (2011) Development of a fluorescein analogue, TokyoMagenta, as a novel scaffold for fluorescence probes in red region. Chem Commun 47:4162–4164
37. Ueno T, Urano Y, Setsukinai K, Takakusa H, Kojima H, Kikuchi K, Ohkubo K, Fukuzumi S, Nagano T (2004) Rational principles for modulating fluorescence properties of fluorescein. J Am Chem Soc 126:14079–14085
38. Bellina F, Cauteruccio S, Montib S, Rossi R (2006) Novel imidazole-based combretastatin a-4 analogues: evaluation of their in vitro antitumor activity and molecular modeling study of their binding to the colchicine site of tubulin. Bioorg Med Chem Lett 16: 5757–5762
39. Bando T, Sugiyama H (2006) Synthesis and biological properties of sequence-specific DNA-alkylating pyrrole − imidazole polyamides. Acc Chem Res 39:935–944
40. Sun YF, Cui YP (2009) The synthesis, structure and spectroscopic properties of novel oxazolone-, pyrazolone- and pyrazoline-containing heterocycle chromophores. Dyes Pigments 81:27–34
41. Peter W, Wilhelm K (2000) Ionic liquids—new "solutions" for transition metal catalysis angew. Chem. Int. Ed 39:3772–3789
42. Kumar A, Kim H-S (2015) *N*-(3-imidazolyl)propyl dansylamide as a selective Hg^{2+} sensor in aqueous media through electron transfer. Spectrochim Acta A 148:250–254
43. Kumar A, Ghosh MK, Choi C-H, Kim H-S (2015) Selective fluorescence sensing of salicylic acids using a simple pyrenesulfonamide receptor. RSC Adv 5:23613–23621
44. Kumar A, Kim H-S (2015) A pyrenesulfonyl-imidazolium derivative as a selective cyanide ion sensor in aqueous media. New J Chem 39:2935–2942
45. Hens A, Maity A, Rajak KK (2014) *N*, *N* coordinating Schiff base ligand acting as a fluorescence sensor for zinc(II) and colorimetric sensor for copper(II), and zinc(II) in mixed aqueous media. Inorg Chim Acta 423:408–420
46. Li ZY, Lin Y, Xia JL, Zhang H, Fan FY, Zeng QB (2011) Synthesis of novel diarylethene compounds containing two imidazole bridge units and tuning of their optical properties. Dyes Pigments 90:245–252
47. Sivaraman G, Chellappa D (2013) Rhodamine based sensor for naked-eye detection and live cell imaging of fluoride ions. J Mater Chem B 1:5768–5772

48. Ding J, Yuan L, Gao L, Chen J (2012) Fluorescence quenching of a rhodamine derivative: selectively sensing Cu^{2+} in acidic aqueous media. J Lumin 132:1987–1993
49. Sivaraman G, Sathiyaraja V, Chellappa D (2014) Turn-on fluorogenic and chromogenic detection of Fe(III) and its application in living cell imaging. J Lumin 145:480–485
50. Magde D, Wong R, Seybold PG (2002) Fluorescence quantum yields and their relation to lifetimes of rhodamine 6G and fluorescein in nine solvents: improved absolute standards for quantum yields. Photochem Photobiol 75:327–334
51. Yin W, Zhu H, Wang R (2014) A sensitive and selective fluorescence probe based fluorescein for detection of hypochlorous acid and its application for biological imaging. Dyes Pigments 107:127–132
52. Zheng H, Zhan X-Q, Biana Q-N, Zhanga X-J (2013) Advances in modifying fluorescein and rhodamine fluorophores as fluorescent chemosensors. Chem Commun 49:429–447
53. Kobayashi H, Ogawa M, Alford R, Choyke PL, Urano Y (2010) New strategies for fluorescent probe design in medical diagnostic imaging. Chem Rev 110:2620–2640
54. Dujols V, Ford F, Czarnik AW (1997) A long-wavelength fluorescent chemodosimeter selective for Cu(II) ion in water. J Am Chem Soc 119:7386–7387
55. Gunnlaugsson T, Leonard JP, Senechal K, Harte AJ (2004) Eu(III)–cyclen–*phen* conjugate as a luminescent copper sensor: the formation of mixed polymetallic macrocyclic complexes in water. Chem Commun:782–783
56. Klein G, Kaufmann D, Schurch S, Reymond J-L (2001) A fluorescent metal sensor based on macrocyclic chelation. Chem Commun: 561–562
57. Katoh R, Suzuki K, Furube A, Kotani M, Tokumaru K (2009) Fluorescence quantum yield of aromatic hydrocarbon crystals. J Phys Chem C 113:2961–2965
58. Kavallieratos K, Rosenberg JM, Chen W-Z, Ren T (2005) Fluorescent sensing and selective Pb(II) extraction by a dansylamide ion-exchanger. Am Chem Soc 127:6514–6515
59. Connors KA Binding Constants: the Measurement of Molecular Complex Stability. New York: Wiley, 1987; pp 21–101; 339–343.
60. Thordarson P (2011) Determining association constants from titration experiments in supramolecular chemistry. Chem Soc Rev 40: 1305–1323
61. Fabbrizzi L, Licchelli M, Pallavicini P, Parodi L (1999) Taglietti A in transition metals in supramolecuar chemistry; sauvage, J. P., Ed. Fluorescent sensors for and with transition metals. John Wiley & Sons Ltd, Chichester
62. Ci YX (1984) Zhou TZ the coordinated complexes in analytical chemistry. Peking University Press, Beijing